Quantitative analysis of ammonium salts in coking industrial liquid waste treatment process based on Raman spectroscopy*

Ya-Nan Cao(曹亚南)[1,2], Gui-Shi Wang(王贵师)[1,†], Tu Tan(谈图)[1,‡], Ting-Dong Cai(蔡廷栋)[3], Kun Liu(刘锟)[1], Lei Wang(汪磊)[1], Gong-Dong Zhu(朱公栋)[1], and Jiao-Xu Mei(梅教旭)[1]

[1] *Anhui Institute of Optics & Fine Mechanics, Chinese Academy of Sciences, Hefei* 230031, *China*
[2] *University of Science and Technology of China, Hefei* 230031, *China*
[3] *College of Physics and Electronic Engineering, Jiangsu Normal University, Xuzhou* 221116, *China*

(Received 4 May 2016; revised manuscript received 26 May 2016; published online 25 August 2016)

Quantitative analysis of ammonium salts in the process of coking industrial liquid waste treatment is successfully performed based on a compact Raman spectrometer combined with partial least square (PLS) method. Two main components (NH_4SCN and $(NH_4)_2S_2O_3$) of the industrial mixture are investigated. During the data preprocessing, wavelet denoising and an internal standard normalization method are employed to improve the predicting ability of PLS models. Moreover, the PLS models with different characteristic bands for each component are studied to choose a best resolution. The internal and external calibration results of the validated model show a mass percentage error below 1% for both components. Finally, the repeatabilities and reproducibilities of Raman and reference titration measurements are also discussed.

Keywords: Raman spectroscopy, wavelet denoising, partial least square regression, ammonium salts

PACS: 74.25.nd **DOI:** 10.1088/1674-1056/25/10/107403

1. Introduction

Over the last few decades, coking liquid waste pollution has always been a major problem throughout the world, especially in China. Coking liquid waste is composed of complex inorganic and organic contaminants such as ammonia, cyanide, sulfate, phenolic compounds, polycyclic aromatic hydrocarbons and polycyclic nitrogen. Most of these pollutants are toxic, refractory, carcinogenic, and usually result in environmental and health problems.[1–4] In China, a mixed catalyst desulfuration technique called HPF is widely utilized in the coking liquid waste treatment process, where HPF is the abbreviation of hydroquinone, phthalocyanine cobalt dualcore sulfonate, and ferrous sulfate. There is still a large quantity of residual ammonium salts (NH_4SCN, $(NH_4)_2S_2O_3$, and $(NH_4)_2SO_4$) among the liquid waste after the desulfuration treatment, which has significant economic values, and can be separated by using a membrane process of nanofiltration.[5] In the separation process, the titration method is commonly employed to find the concentration information of ammonium salts, which is time-consuming (dozens of minutes or more), manually operated and impossible to detect two components simultaneously. Consequently, there is a strong demand for instantaneous, autonomous analytical methods to provide species identification and accurate measurements.

Raman spectroscopy has proven itself to be a powerful tool for the study of various fields of science, primarily due to the extraordinary versatility of sampling methods. Raman spectroscopy gives the detailed vibration spectrum of the analyte, which can be treated as its "molecular fingerprint", and allows easy explanation and identification. Over the last years, there has been a tremendous technical improvement in Raman spectroscopy, such as in fluorescence, sensitivity or reproducibility.[6–12] These advances, together with the ability of Raman spectroscopy to examine aqueous samples inside glass containers, meet our demand perfectly. Moreover, Raman spectroscopy has been successfully verified as a viable tool for the rapid detection of nitrate and nitrite in water and liquid waste.[13]

In the present work, a compact commercial Raman spectrometer- (QE-pro, Ocean Optics, Inc.) based detection system is proposed for the quantitative analysis of the ammonium salts in the coking industrial liquid waste treatment process. Here, Raman spectra of industrial liquid waste with different mixing ratios of ammonium salts are recorded, and titration measurements are performed parallelly for reference analysis. Moreover, for eliminating the influence of laser power disturbance and improving the detection accuracy, wavelet filtering and the so-called internal reference standard calibration strategy are implemented in data preprocessing. Then, all the processed data are analyzed by using the partial least square (PLS) method.

*Project supported by the National Natural Science Foundation of China (Grant Nos. 41405022 and 61475068).
†Corresponding author. E-mail: gswang@aiofm.ac.cn
‡Corresponding author. E-mail: tantu@aiofm.ac.cn
© 2016 Chinese Physical Society and IOP Publishing Ltd

2. Experiments

2.1. Samples and reference analysis

Forty-two samples from different distillation stills in the separation processes were recorded in Suzhou Jiuwang Multiple Ammonium Salts Technology Company Ltd. from October 2014 to March 2015, with the concentrations (mass percentage) of NH_4SCN ranging from 16% to 64%, $(NH_4)_2S_2O_3$ from 12% to 55%, and $(NH_4)_2SO_4$ below 2%, respectively, each sample was analyzed by using the titration method. For covering the whole concentration range of the industrial process, twenty-one artificially synthesized samples were prepared by using pure samples and industrial samples. These pure samples were also utilized to validate the spectrum information of ammonium salts. In order to validate the PLS based prediction models, twenty-four samples were collected for the external validation from May to August 2015. It should be noted that sulfur particles in the samples needed filtering firstly, and then the samples were diluted uniformly to 50 mL with deionized water for further titration measurement and Raman analysis.

2.2. Instrumentation and spectra acquisition

A compact QE-pro series Raman detection system was employed in this investigation (Fig. 1).

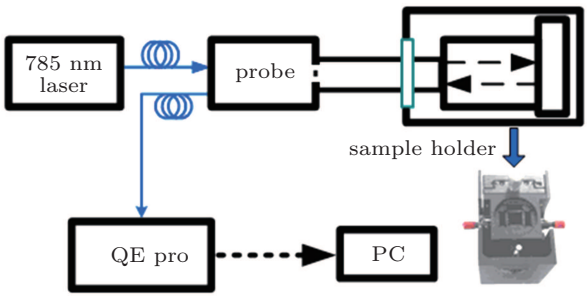


Fig. 1. (color online) Schematic diagram of experimental set-up.

An SMA-coupled and spectrum stabilized multi-mode 785-nm laser with a maximum power of 350 mW (300 mW was chosen in the experiment) and a spectral line width of 0.2 nm was used as an excitation light source. The output beam illuminated the samples contained in a cuvette vertically via a bifurcated optical probe with one leg coupled to the laser and the other to a QE-pro Raman spectrometer. By the same probe, the back-scattered Raman beam was collected by the QE-pro spectrometer with an integration time of 20 s. The QE-pro spectrometer is responsible from 200 nm to 1100 nm with an optical resolution about 5 cm^{-1} and can be cooled down to -15 °C with the on-board TE-Cooler to reduce dark noise. Finally, the Raman spectra were acquired by an omnidriver-(dll files were provided by Ocean Optics) based Lab-view program or Ocean View (Ocean Optics, Inc.) with dark spectrum subtraction and wavelength correction performed during the acquisition. In particular, in order to minimize the influences of temperature and humidity change, the whole system was placed in a chamber with constant temperature (20 ± 1 °C) and humidity (RH $45 \pm 1\%$).

2.3. Theory

The intensity of Raman scattering can be presented in simple form as

$$R = IKP\sigma C, \tag{1}$$

where R is the Raman peak intensity, I is the laser intensity, K includes instrument parameters such as optical transmission and collection efficiency, P is the sample path length, σ is the Raman cross-section or scattering efficiency of the species under investigation, and C is the concentration per unit volume. As parameters such as K, I, and P may change during the experiment, an internal reference standard is often required.[14,15] In this experiment, the entire spectrum was normalized by multiplying a factor N

$$N = A/R_{H_2O}, \tag{2}$$

where R_{H_2O} is the peak intensity of a water spectrum and A is an arbitrary constant, then the normalized form of the sample and water can be obtained, respectively,

$$R^*_{\text{sample}} = NIKP\sigma_{\text{sample}}C_{\text{sample}}, \tag{3}$$

$$R^*_{H_2O} = NIKP\sigma_{H_2O}C_{H_2O}, \tag{4}$$

where R^* indicates the normalized peak intensity. Because the spectra of the sample and water are acquired simultaneously, the term $NIKP$ in Eq. (3) is the same as that in Eq. (4). Thus the following relation can be obtained:

$$R^*_{\text{sample}} = B * \left(\frac{C_{\text{sample}}}{C_{H_2O}}\right), \tag{5}$$

where B is constant across all measurements for different samples. Equation (5) indicates that the normalized peak intensity of the sample is directly proportional to the ratio of the concentration of the sample to that of the water. Considering that the concentration of water can be regarded as a constant, the normalized peak intensity of the sample is proportional to its concentration regardless of the variance of the term IKP in Eq. (4). In the present paper, a characteristic peak of water is employed as the internal reference standard to normalize the spectrum, which shows distinct improvement in our experiment.

3. Results and discussion

3.1. Raman spectroscopy results

In order to validate the spectral information of different ammonium salts, Raman spectra of pure samples are recorded (Fig. 2).

By comparing the spectra of studied compounds with those of deionized water, we can observe the characteristic peaks of NH_4SCN at 754 cm^{-1} and 2070 cm^{-1}, peaks of $(NH_4)_2S_2O_3$ at 340, 449, 670, 994, and 1122 cm^{-1}, and the peaks of $((NH_4)_2SO_4)$ at 452, 619, 989, and 1115 cm^{-1}. Note that the characteristic peaks of $(NH_4)_2S_2O_3$ and $(NH_4)_2SO_4$ come in a pair and overlap with each other. Normally, multi-peak fitting algorithms can be employed to obtain their concentrations. However, considering that the concentration range of $(NH_4)_2SO_4$ is below 2%, and its concentration is difficult to obtain accurately by using the reference titration measurement, the analysis of $(NH_4)_2SO_4$ is not included in this paper. Here the method we used to minimize the prediction bias caused by $(NH_4)_2SO_4$ is to choose the best spectrum characteristic band of $(NH_4)_2S_2O_3$ to build prediction models.

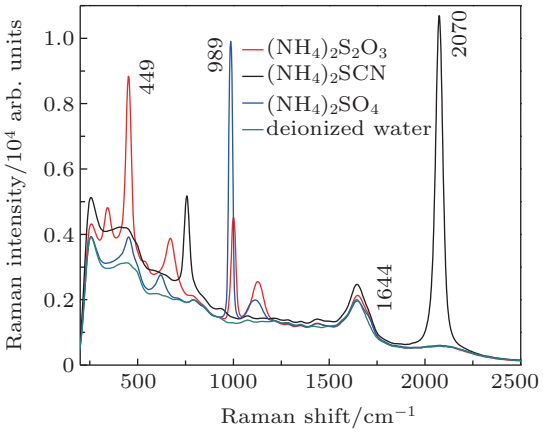


Fig. 2. (color online) Raman spectra of pure components and deionized water.

The characteristic bands of samples for internal calibration are shown in Fig. 3, where two characteristic bands of NH_4SCN (blue), five characteristic bands of $(NH_4)_2S_2O_3$ (pink) and two characteristic bands of water (gray) are marked with different symbols. First, these characteristic bands were quantitatively studied by using the PLS regression after wavelet denoising and an internal normalizing process. Then, the best prediction model can be identified.

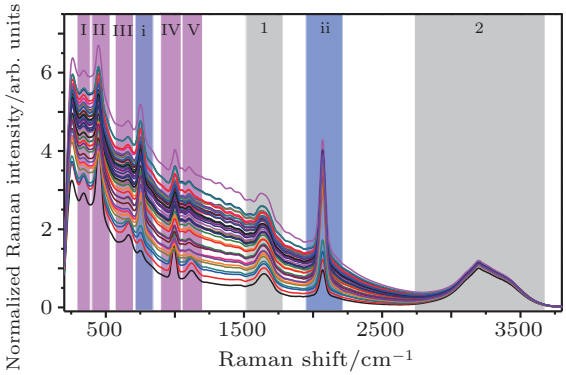


Fig. 3. (color online) Spectra of the calibration samples and their characteristic bands, (NH_4SCN i and ii, $(NH_4)_2S_2O_3$ *I*–*V*, water vapor 1 and 2).

3.2. Data preprocessing and software

Data preprocessing is always an important procedure for Raman-based investigations, which may make the analysis more accurate and improve the detection limit. Wavelet transform is proven to be a powerful tool in analyzing Raman spectra and details have already been described elsewhere.[16–19] Here only the process is presented. For reducing the unwanted noise, a db02 wavelet-transform-based denoising method is employed, which can produce much higher denoising quality than conventional methods and retain the details of a signal after denoising. The comparison between denoised signals and raw data is shown in the inset of Fig. 4(a), with an offset added on the denoised data.

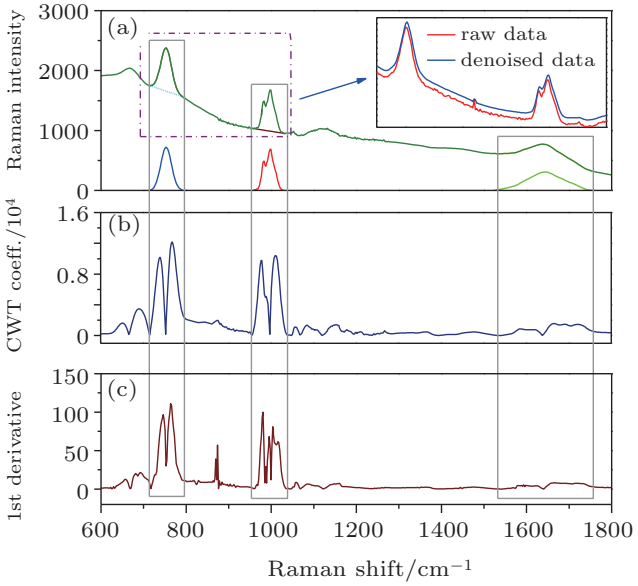


Fig. 4. (color online) Data preprocessing results for a sample: (a) spectra results after background removal, comparison between wavelet denoised results and raw spectra data (inlet). (b) Continuous wavelet transform (CWT) coefficients for the denoised spectra signal. (c) The 1st derivative results of the denoised spectra signal.

It can be seen from the graph that the signal-to-noise ratio is significantly improved. As for normalizing the spectrum, characteristic band 2 of water (Fig. 3) is utilized as an internal reference standard, owing to the higher signal-to-noise ratio and more stable than that in region 1. In order to obtain the peak value of water, continuous wavelet transform (CWT) coefficients (Fig. 4(b)) are employed as the reference signal to find the starting and ending point of the validated peaks, which shows more rigorous than normally used derivative methods (Fig. 4(c)). Finally, the normalized spectrum is calculated after dividing the raw spectrum by the peak value of water.

It should be noted that the programs used for data preprocessing are compiled in laboratory virtual instrument engineering workbench (LabVIEW) environment, the wavelet transform is implemented by virtue of Wavelet analysis Toolkits (National Instruments Corp.), and the PLS analysis is performed with TQ Analyst (Thermo Fisher Scientific).

3.3. Quantitative analysis

3.3.1. PLS models and internal validation

Quantitative analysis is performed on 87 samples including industrial and artificially synthesized samples. Sixty three samples, 42 industrial and 21 synthetic, collected from October 2014 to March 2015, are randomly divided into two sets to form a calibration set and an internal validation set for the PLS models. After that, an external validation is conducted on 24 industrial samples collected from May to August 2015.

The calibration results for a PLS model are explained in terms of correlation coefficient (R), root mean square error of calibration (RMSEC), root mean square error of prediction (RMSEP), and the number of factors. Comparisons among the PLS models employing different smoothing methods are shown in Table 1.

Table 1. PLS models with different data processing methods.

Samples and models	R	RMSEC	RMSEP(In)*	Factors
NH_4SCN				
PLS-raw*	0.99623	0.0365	0.0395	5
PLS-ND*	0.99584	0.0383	0.0562	4
PLS-SG*	0.99608	0.0372	0.0393	5
PLS-WL*	0.99735	0.0306	0.0383	5
PLS-WLN*	0.99876	0.0192	0.0361	3
$(NH_4)_2S_2O_3$				
PLS-raw	0.98754	0.0495	0.0804	3
PLS-ND	0.98488	0.0545	0.0874	2
PLS-SG	0.98716	0.0503	0.0812	3
PLS-WL	0.99541	0.0301	0.0458	3
PLS-WLN	0.99663	0.0258	0.0299	3

* -raw: raw data, -ND: Norris derivative filter, -SG: Savitzky–Golay filter, -WL: wavelet denoising, -WLN: normalized data after wavelet denoising, RMSEP(In): RMSEP of internal calibration.

The smoothing methods considered here include Norris derivative filter (-ND), Savitzky–Golay filter (-SG), wavelet denoising (-WL), and wavelet denoising combined with the water normalization (-WLN). For NH_4SCN, where characteristic band ii is chosen for the comparison, the correlation coefficient R of PLS-WL is slightly better than the results of PLS-ND and PLS-SG, and R is further improved by using PLS-WLN. Actually, each method shows a good correlation with the reference analysis, and the low RMSEC and RMSEP values indicate good prediction of the samples. As for $(NH_4)_2S_2O_3$ (region IV is used), the R is significantly improved while the wavelet denoising is employed, and the calibration results are further optimized when the water optimization is performed. Accordingly, the PLS-WLN is chosen as the final prediction model for both samples. Note that the calibration results of NH_4SCN is better than $(NH_4)_2S_2O_3$, it is mainly because the peak of NH_4SCN has a higher signal-to-noise ratio and there is no other interference near the characterizing band of NH_4SCN.

3.3.2. Accuracy of the models (external validation)

In order to evaluate the predicting ability of PLS–WLN models, 24 samples from industrial process are tested from May to August in 2015. Table 2 presents the results of each sample in different regions, where two NH_4SCN bands and five $(NH_4)_2S_2O_3$ are considered.

Table 2. PLS–WLN models for different spectrum regions and external validation results.

Samples and regions	R	RMSEC	RMSEP(Ex)*	Factor
NH_4SCN				
Region i	0.99785	0.0252	0.166	2
Region ii	0.99876	0.0192	0.040	3
$(NH_4)_2S_2O_3$				
Region I	0.99290	0.0359	0.063	4
Region II	0.99309	0.0354	0.033	1
Region III	0.99582	0.0276	0.037	4
Region IV	0.99663	0.0258	0.128	2
Region V	0.99602	0.119	2	

*RMSEP(Ex): RMSEP of external calibration.

For NH_4SCN, the calibration results are almost the same for both regions except the RMSEP(ex) (RMSEP of external calibration). The main reason for the RMSEP(ex) of region i (0.166) being larger than region ii (0.04) is that the region ii obtains higher signal-to-noise ratio and there is an interference from $(NH_4)_2S_2O_3$ near region i which makes the background of region i irregular and may cause overfitting. Therefore, PLS–WLN mode using region ii is validated for the prediction of NH_4SCN. For $(NH_4)_2S_2O_3$, the RMSEP(ex) results of regions II and III are similar to their RMSEC results, while the RMSEP(ex) results of regions I, IV, and V up to 0.063, 0.128, and 0.119 are obtained, respectively. This result indicates that the interference from $(NH_4)_2SO_4$ with low concentration (below 2%) can be ignored in regions II and III. Figures 5 and 6 show the external calibration results of NH_4SCN and $(NH_4)_2S_2O_3$ by using region ii and region II, respectively.

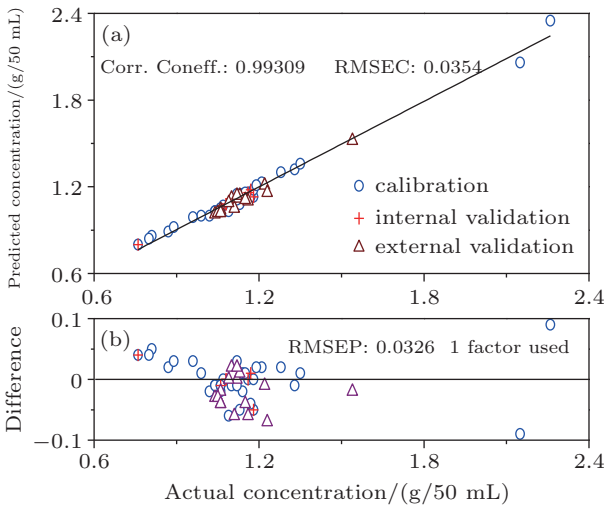


Fig. 5. (color online) External calibration results for NH_4SCN using region ii.

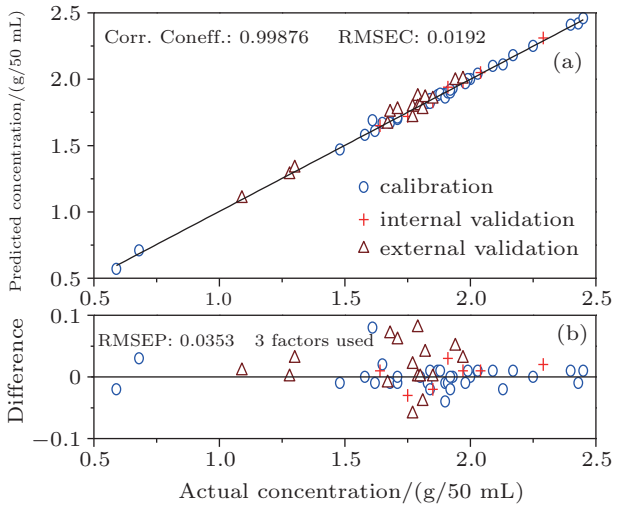


Fig. 6. (color online) External calibration results for $(NH_4)_2S_2O_3$ using region II.

For each sample, the prediction error is calculated by the difference between the prediction result and the reference titration result. Finally, a mass percentage error below 1% for both samples is obtained.

3.3.3. Repeatability and reproducibility of methods

Repeatability of reference titration method and Raman technique are studied by using the same industrial sample. One thousand successive measurements with 20-s interval are performed to estimate the repeatability of Raman technique. Figure 7 shows a result of successive measurements with the mean value and standard deviation of 1.693 ± 0.027 for NH_4SCN and 2.945 ± 0.025 for $(NH_4)_2S_2O_3$, respectively.

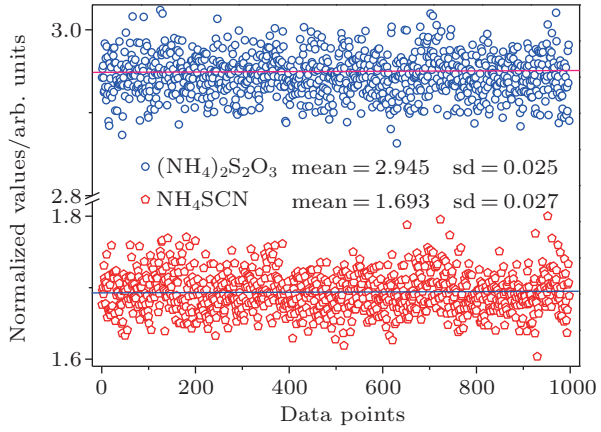


Fig. 7. (color online) Results of 1000 successive measurements with 20-s interval for $(NH_4)_2S_2O_3$ and NH_4SCN.

For uniformity, the standard deviation is expressed as mass percentage error (MPE). The MPEs of NH_4SCN and $(NH_4)_2S_2O_3$ for Raman technique are 0.3% and 0.25%, respectively. The repeatability estimation of the reference titration method is performed five times over one day with one operator. The MPEs of both components for the reference titration method are below 0.2%.

The reproducibility study of reference titration method is conducted five times per day by using the same sample with 3 operators during one week. The MPEs of both components are 0.4%, which is larger than the repeatability estimation result. Reproducibility study of Raman technique is performed with 100 successive measurements recorded per day and by three operators during one week. The standard derivation expressed as MPE is around 0.28% for both components. All results mentioned above guarantee that the prediction results of Raman results are credible.

4. Conclusions

Rapid measurements of NH_4SCN and $(NH_4)_2S_2O_3$ in the coking liquid waste treatment processes are performed by employing a compact Raman detection system with an integration time of 20 s. Firstly, comparisons among different smoothing methods are analyzed by using PLS. The results show a distinct improvement when wavelet filtering and an internal normalization are employed in data preprocessing. Then PLS models with different regions for both components are also analyzed. It is found that region ii of NH_4SCN and regions II and III of $(NH_4)_2S_2O_3$ have higher correlation with reference titration measurements and lower RMSEP(ex). In summary, this Raman detection system shows that it is a promising powerful tool for not only recognizing the three kinds of ammonium salts but also monitoring the process of liquid waste treatment processes and purity detection of finished products.

Acknowledgement

We thank Zhijie Gu and Chen Qing from Suzhou Jiuwang Multiple Ammonium Salts Technology Company Ltd. for supplying the samples and titration measurements.

References

[1] Cheng S 2003 *Environmental Science and Pollution Research* **10** 192
[2] Wang M, Webber M, Finlayson B and Barnett J 2008 *Journal of Environmental Management* **86** 648
[3] Pal P and Kumar R 2014 *Separation & Purification Reviews* **43** 89
[4] Du J B, Tang Y L and Long Z W 2012 *Acta Phys. Sin.* **61** 153101 (in Chinese)
[5] Yin N, Yang G, Zhong Z X and Xing W H 2011 *Desalination* **268** 233
[6] Das R S and Agrawal Y K 2011 *Vibrational Spectroscopy* **57** 163
[7] Clarke R H, Londhe S and Premasiri W R 1999 *Journal of Raman Spectroscopy* **30** 827
[8] Premasiri W R, Clarke R H, Londhe S and Womble M E 2001 *Journal of Raman Spectroscopy* **32** 919
[9] Malka I, Petrushansky A, Rosenwaks S and Bar I 2013 *Appl. Phys. B* **113** 511
[10] Sowoidnich K and Kronfeldt H D 2012 *Appl. Phys. B* **108** 975
[11] Breitenbach J, Schrof W and Neumann J 1999 *Pharmaceutical Research* **16** 1109
[12] Strachan C J, Rades T, Gordon K C and Rantanen J 2007 *Journal of Pharmacy and Pharmacology* **59** 179
[13] Ianoul A, Coleman T and Asher S A 2002 *Anal. Chem.* **74** 1458
[14] Kudelski A 2008 *Talanta* **76** 1
[15] Dunk R M, Peltzer E T, Walz P M and Brewer P G 2005 *Environmental Science & Technology* **39** 9630
[16] Baek S J, Park A, Kim J, Shen A and Hu J 2009 *Chemometrics and Intelligent Laboratory Systems* **98** 24
[17] Chen D, Chen Z and Grant E 2011 *Anal. Bioanal. Chem.* **400** 625
[18] Hu Y, Jiang T, Shen A, Li W, Wang X and Hu J 2007 *Chemometrics and Intelligent Laboratory Systems* **85** 94
[19] Li Z, Zhan D J, Wang J J, Huang J, Xu Q S, Zhang Z M, Zheng Y B, Liang Y Z and Wang H 2013 *Analyst* **138** 448